Supporting Information

Fluorescence-activated cell sorting of human L-asparaginase mutant libraries for detecting enzyme variants with enhanced activity

Christos S. Karamitros[1] and Manfred Konrad

Enzyme Biochemistry Group, Max-Planck Institute for Biophysical Chemistry, Göttingen, D-37077, Germany

[1]**Present address:** University of Texas at Austin, Department of Chemical Engineering, 2500 Speedway, Austin, Texas, TX 78712-1095.

Table S1. Oligonucleotide primers used in this study. Restriction enzyme recognition sites are shown in italics (NdeI site for the 5' site, *CATATG*, and BamHI site at the 3' site, *GGATCC*).

Primer	Sequence
$FW_{hASNase3}$wt	GGAATTC*CATATG*AATCCCATCGTAGTGGTCCACGGCGGCGG
$RV_{hASNase3}$wt	CGC*GGATCC*TTAGGGAAGGTCGGTGATAGTAGTATCGTCAG
FW_SSM-Lib1	ACCTCCACAGGCGGT**NNSNNS**AATAAAATGGTCGGCCGC
RV_SSM-Lib1	GCGGCCGACCATTTTATT**SNNSNN**ACCGCCTGTGGAGGT
FW_SSM-Lib2	CTGGTGACAGAG**NNS**AACAAAAAG**NNS**CTGGAAAAAGAG
RV_SSM-Lib2	CTCTTTTTCCAG**SNN**CTTTTTGTT**SNN**CTCTGTCACCAG

Primer	Sequence
FW_SSM-Lib3	GGAATTC*CATATG*AATCCC**NNSNNSNNSNNS**CACGGCGGCGGAGCCGGTC
RV_SSM-Lib3	GACCGGCTCCGCCGCCGTG**SNNSNNSNNSNN**GGGATTCATATGGAATTCC
FW_SSM-Lib4	TAATAAA**NNSNNS**GGCCGCGTTGGGGACTCACCG**NNSNNS**GGAGC
RV_SSM-Lib4	GCTCC**SNNSNN**CGGTGAGTCCCCAACGCGGCC**SNNSNN**TTTATTA

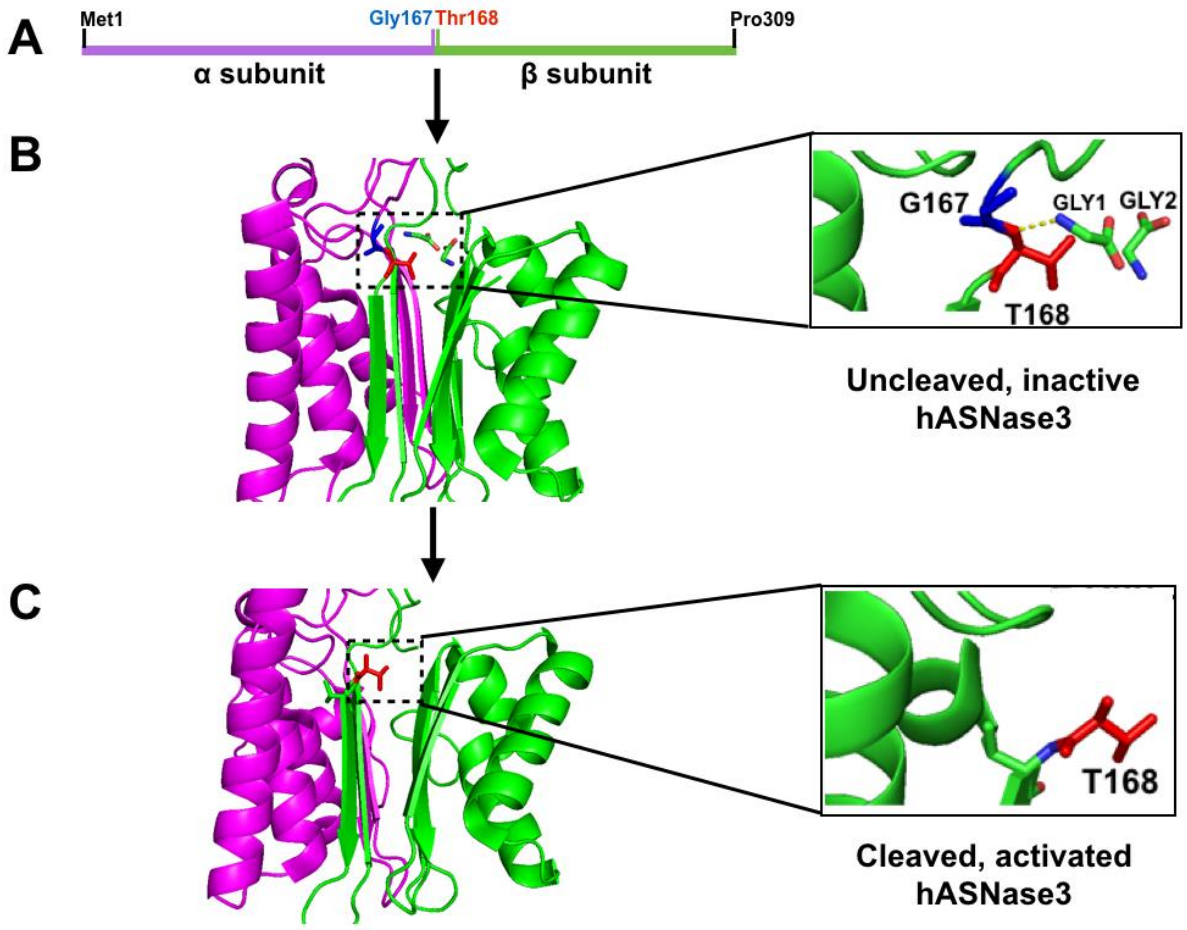

Figure S1. Structural schemes representing intramolecular processing of hASNase-3. Part (A) shows the full-length inactive enzyme species. With magenta is labeled the α subunit and with green the β subunit. Residues Gly167 and Thr168, which are critical for intramolecular processing, are labeled blue and red, respectively. Parts (B) and (C) show the interaction between two free glycine molecules (accelerators for autocatalytic activation)[1] and the enzyme's active site, and the final active enzyme species, respectively.

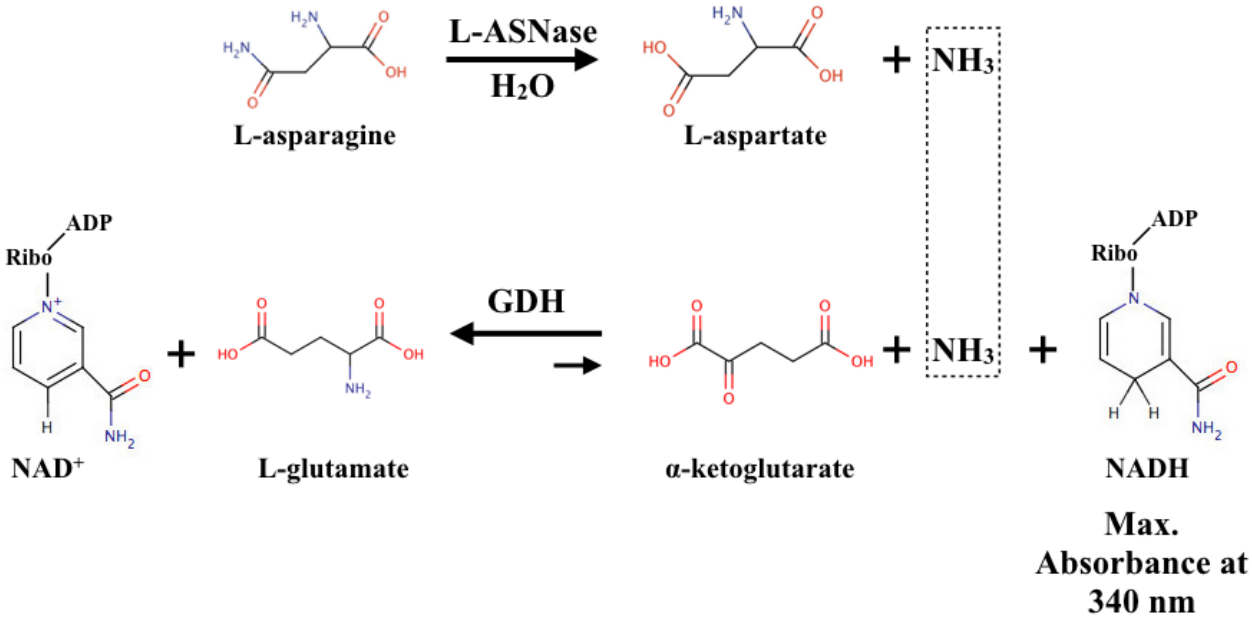

Figure S2. The NADH-dependent coupled-enzyme assay, which was employed for the kinetic characterization of hASNase-3 and its variants. The produced ammonia of the L-ASNase reaction is coupled to a second reaction where NADH and α-ketoglutarate are utilized by glutamate dehydrogenase (GDH) which plays the role of the helper enzyme. The L-ASNase activity is proportional to the production of ammonia and this, in turn, is proportional to the oxidation of NADH which is monitored spectrophotometrically as a decrease of absorbance at 340 nm.

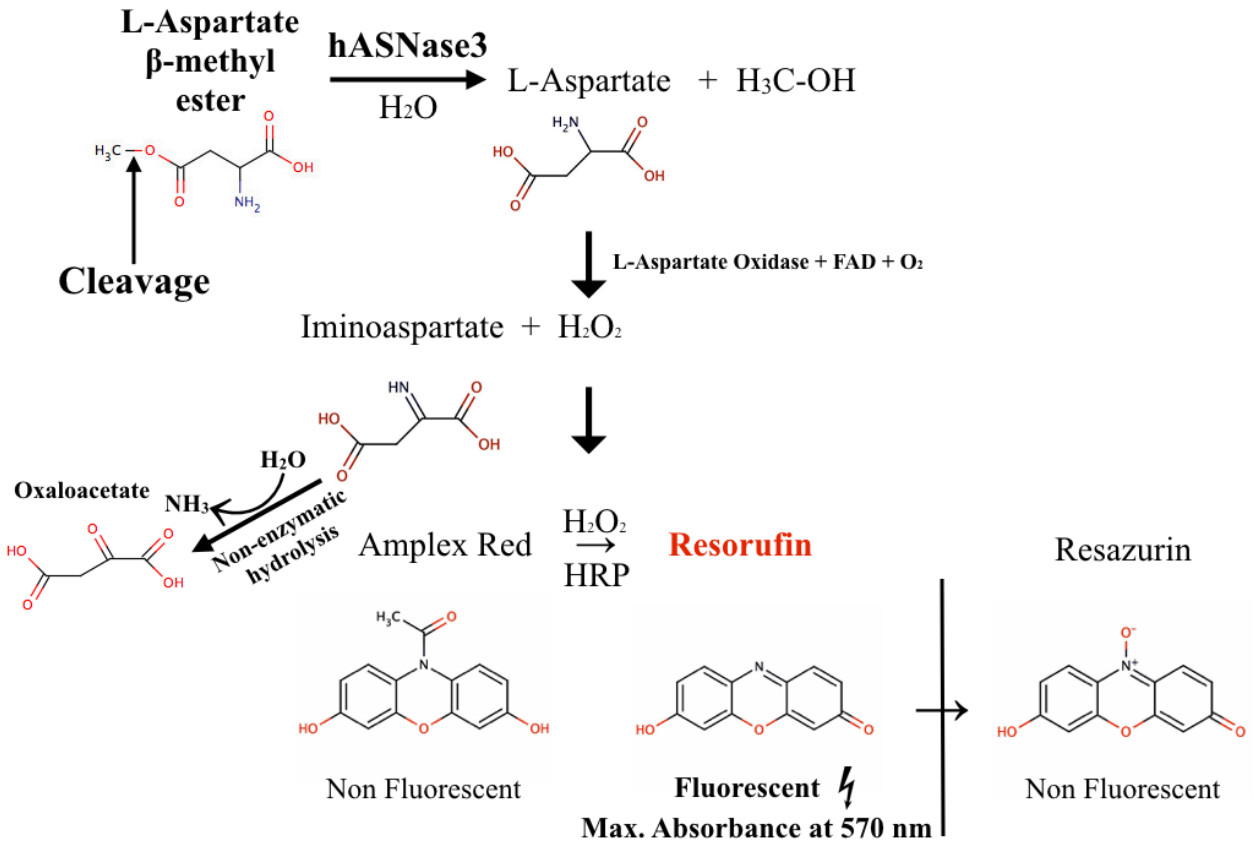

Figure S3. The three-step coupled-enzyme assay we have developed[2] for the recording of L-ASNase activities in either the fluorescence or the absorbance mode. In the present study, this assay was employed for the detection of catalytically improved hASNase-3 variants after the final FACS sorting step using L-Asn as substrate in 96-well plate format (fluorescence mode), as well as for the steady-state kinetic characterization of the variants using L-Asp-β-methyl-ester as substrate in the absorbance mode (570 nm). Note that iminoaspartate can non-enzymatically be hydrolyzed to oxaloacetate and ammonia.[3] For more details regarding the assay conditions, see main text.

Genetic complementation and validation of the FACS screening approach for detecting L-asparaginase activity using the JC1(DE3) 5-gene-deletion *E. coli* strain.

Genetic complementation of the 5-gene-deletion JC1(DE3) *E. coli* strain deficient in L-aspartate biosynthesis was validated by expressing five L-ASNases that display significantly different activities (with respect to both k_{cat} and K_M) as L-asparagine-hydrolyzing enzymes. The following genes (coding regions) were cloned in the plasmid pET14b-SUMO: human L-ASNase-1 (hASNase-1)[4], human L-ASNase-3 (hASNase-3)[5,6], *E. coli* ASNase-1 (*Ec*ASNase-1)[7], *E. coli* ASNase-2 (*Ec*ASNase-2; therapeutically used enzyme)[8], and *S.cerevisiae* ASNase-1 (*Sc*ASNase-1).[9,10] The plasmid with no L-ASNase insert was also included in this series of experiments in order to evaluate the background growth of the bacterial cells. Cells were transformed with equal

amounts of DNA, plated on M9 minimal medium agar plates supplemented with all amino acids except from L-Asp, 1mM IPTG to induce the expression of the L-ASNases, and with all other compounds as described in the Methods section, and then incubated at 37℃. Eventually, colony formation - though of highly variable colony sizes - was observed in all cases of transformations with the plasmids encoding different ASNases after ~ 30 hours of incubation indicating positive genetic complementation. The plates with the negative control (plasmid with no insert) showed very small pinpoint colonies, possibly due to the presence of L-Asp traces in the stocks of the other amino acids, or due to spontaneous hydrolysis of L-Asn, which provided the basal level for initial cell growth. On the other hand, when the same experiment was carried out in liquid cultures with M9 minimal medium, after 24 hours of incubation at 37℃, the negative control showed no cell growth (non-detectable OD_{600} change), while the positive controls grew normally exhibiting an OD_{600} ~ 1.

The next validation step of the screening system included a quantitative comparison of hASNase-3 and *Ec*ASNase-2 expression using the FACS system before starting the actual screening of the generated hASNase-3 mutant libraries. This experiment aimed to determine the fluorescence mean of the cell population which can be obtained from cells expressing two enzymes with very distinct catalytic properties: hASNase-3 displays a k_{cat}/K_M ~ 300 $M^{-1}s^{-1}$, while *Ec*ASNase-2 ~ $6x10^5$ $M^{-1}s^{-1}$ (kinetic constants determined by applying the NADH-dependent assay at 25℃) which means that the *E.coli* enzyme is ~ 2,000-fold more efficient. To this end, cells transformed with hASNase-3 and *Ec*ASNase-2 harboring in parallel the pBAD33-eGFP plasmid, were prepared for FACS analysis as described in the Methods section above, and their fluorescence profile was recorded. **Figure S4** shows the result of this experiment.

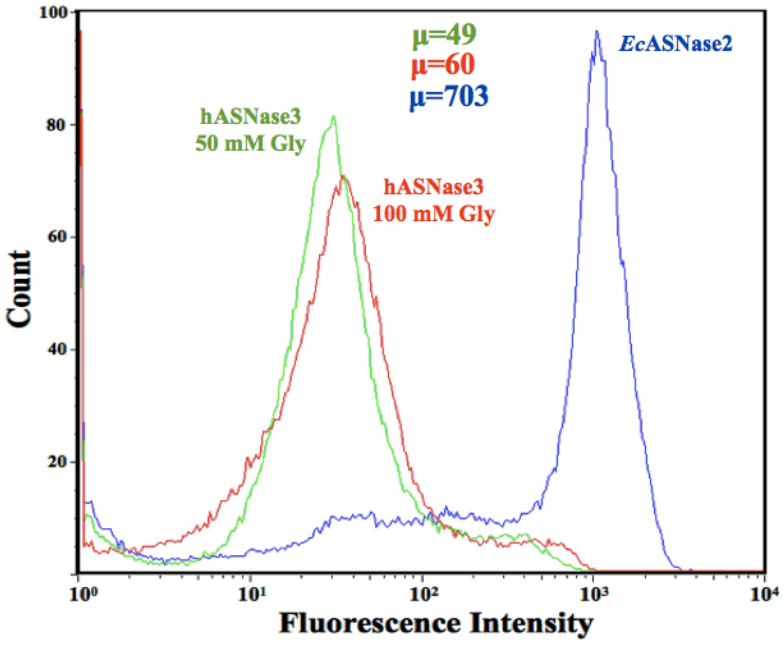

Figure S4. FACS fluorescence profiles obtained for hASNase-3- and *Ec*ASNase-2-dependent genetic complementation in the *E. coli* strain JC1(DE3) which is deficient for L-aspartate biosynthesis. Two concentrations of glycine (50 and 100 mM) were added to the growth medium to test for efficiency of inducing the activation of hASNase-3 intramolecular processing; they showed similar fluorescence profiles. With μ is denoted the arithmetic fluorescence mean.

The results revealed that while the *in-vitro* catalytic efficiencies of the two enzymes differ about 2000-fold, the genetic complementation assay using the eGFP as reporter protein showed only ~ 20-fold difference in their fluorescence means. This may be attributed to saturated expression levels of eGFP in case of *Ec*ASNase-2 expression, or the utilization of the produced L-Asp for other cellular processes, thereby not reflecting in quantitative terms the actual catalytic differences between the two enzymes. Perhaps the fluorescence profile of another L-ASNase considerably more efficient than *Ec*ASNase-2 (such as the enzyme from *Erwinia chrysanthemi*) would provide more information about the upper limit of the applied screening system. Treatment with glycine using concentrations of 50 and 100 mM, respectively, resulted in similar fluorescence means. Prior *in-vitro* incubation experiments have shown that the activation of hASNase-3 is induced by glycine in a concentration-dependent manner.[1] The FACS results obtained here can be explained by assuming similar glycine uptake by the *E.coli* cells at either concentration tested. Thus, the cells may take up from their growth medium a certain amount of glycine which saturates at concentrations lower than 50 mM. As we observed that cells grew somewhat slower in the presence of 100 mM glycine, for the next screening experiments 50 mM was used as standard glycine concentration.

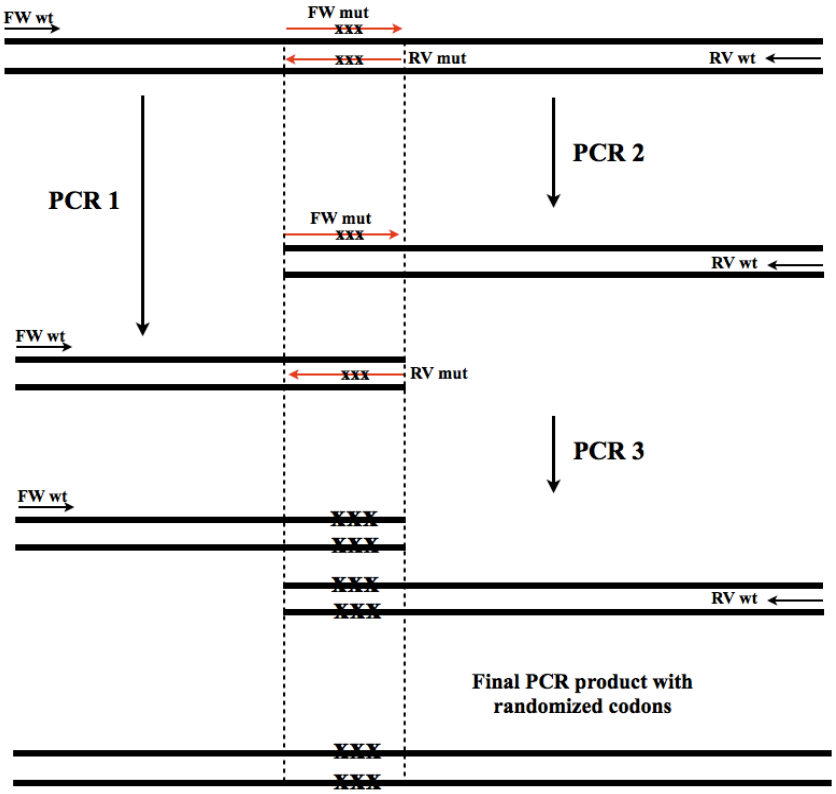

Figure S5. Overlap extension PCR method used for site-saturation mutagenesis. This method consists of three successive amplification steps and involves four primers: two external ones which cover the 5'- and 3'- ends of the wildtype sequence (designated as forward FW wt and reverse RV wt, respectively), and two additional ones which carry the desired degenerate codons (NNS) to be incorporated in the final sequence (indicated by red arrows in the figure; xxx denotes the nucleotide mismatches). Two independent PCR reactions (PCR 1 and PCR 2) amplify two fragments which overlap at the regions flanking the mismatches. In a final third step, the two amplified fragments are combined in equal molar quantities with the initial external wildtype primers and are subjected to the last PCR reaction resulting in the final amplicon that carries the degenerated codons, or point mutations. The number of nucleotides upstream and downstream of the mismatch codons is very critical for the success of this mutagenesis method, since these overhangs determine the annealing efficiency of the long fragments generated by the first two PCRs. The overlap regions should encompass at least fifteen, or more, nucleotides depending on the number of codons which are to be randomized.

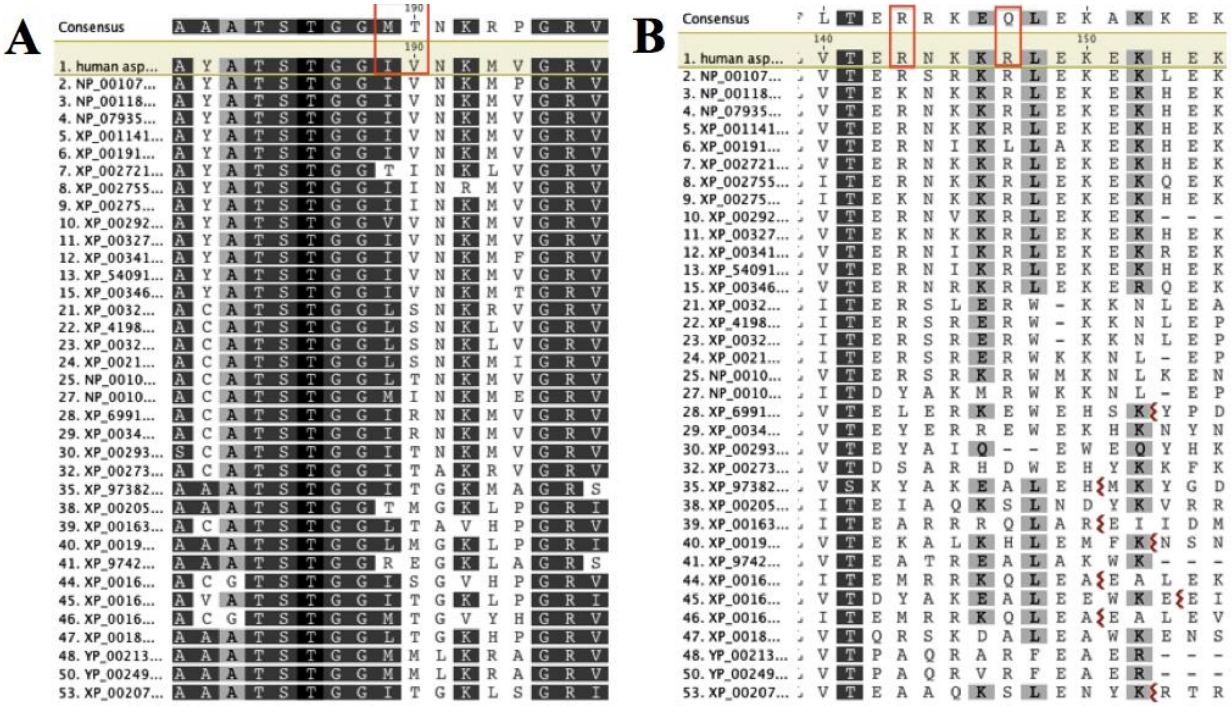

Figure S6. Massive amino acid sequence alignment of 1000 hASNase-3 homologues (here are shown only the first 50) from different organisms. The first line corresponds to hASNase-3 (number 1), and on the top of the alignment the consensus residues for each amino acid position are shown. Red-framed are the two amino acids which were randomized for either SSM library, i.e. I189 and V190 for SSM-Lib1 (A), and R143 and R147 for SSM-Lib2 (B). The alignment shows that none of the selected residues is fully conserved among L-ASNases. The alignment was performed by using the Geneious program.

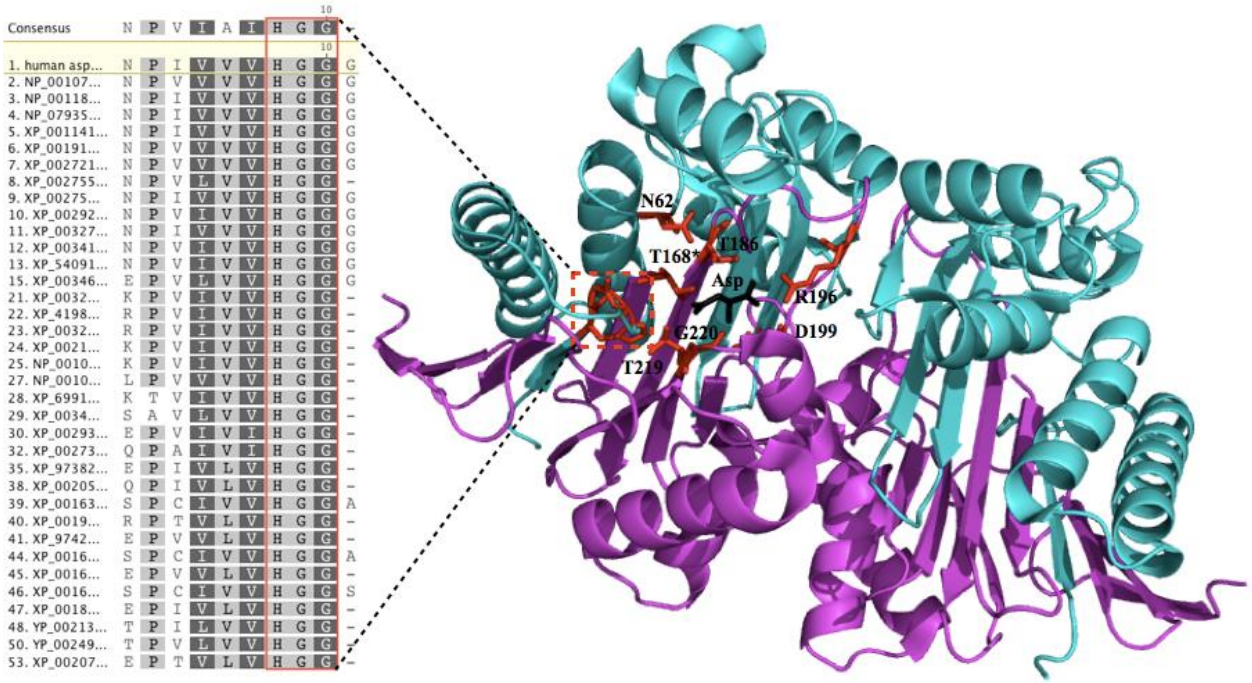

Figure S7. Structure of wildtype hASNase-3. In this structural model, the α subunit is colored in cyan, and the β subunit in magenta. Black-labeled is the product of the enzymatic reaction, L-Asp. Red-labeled are the residues which constitute the catalytic centre of the enzyme and are directly involved in substrate binding: Asn62, Thr186, Arg196, Asp199, Thr219, Gly220, and the catalytic threonine Thr168* which plays the pivotal role of the nucleophile. In the figure is also shown a short stretch of the sequence alignment of the homologous enzymes similar to Fig. S3. In the structure, three amino acids are framed by a red square represent the amino acid triad His8-Gly9-Gly10. Structural analysis had shown that this triad is crucial for the enzyme's autoproteolytic activation and catalysis. The alignment makes evident that these residues are highly conserved among all homologs from different organisms. The structural representation was prepared by PyMol using the structure of fully cleaved hASNase-3 (pdb entry: 4HLP).

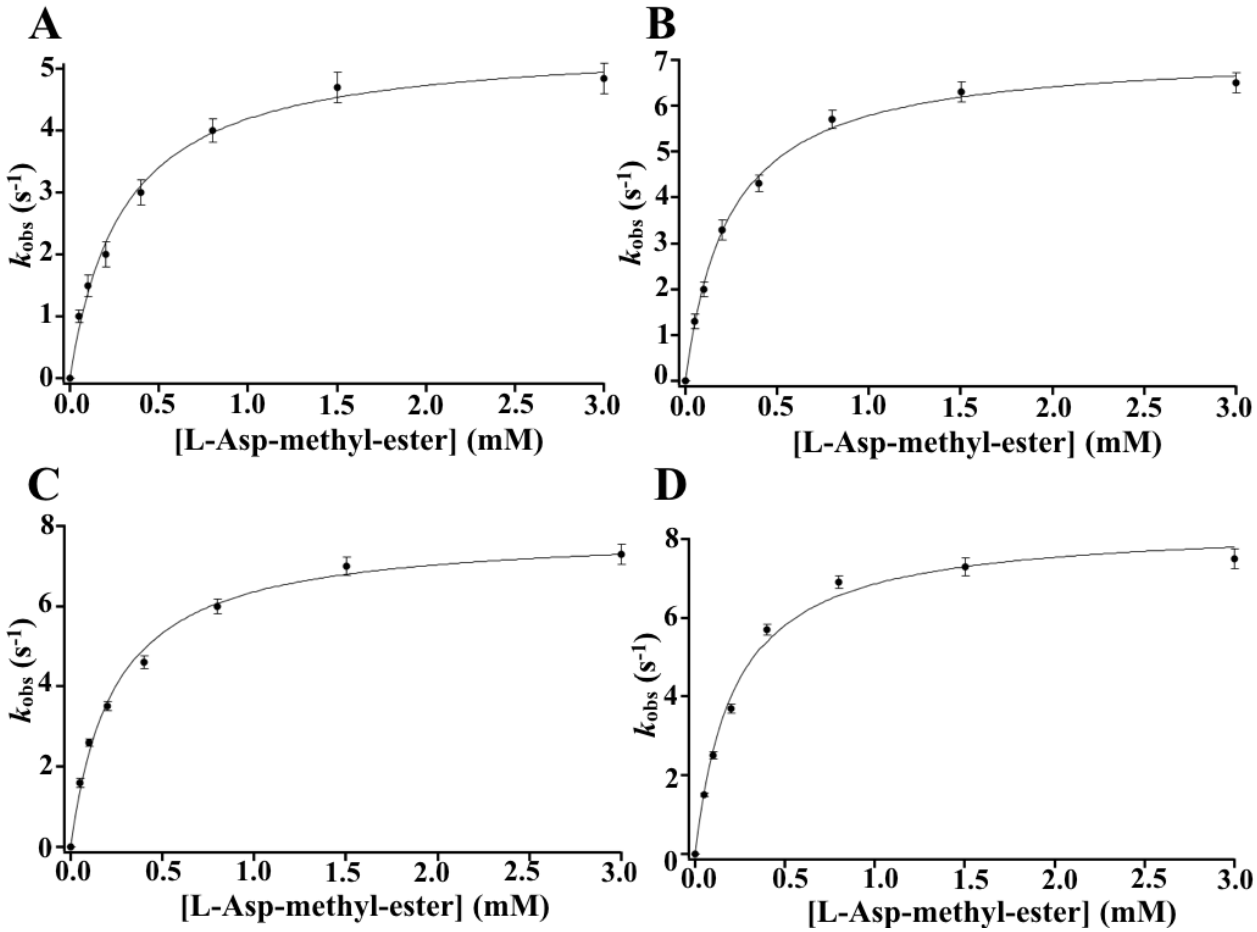

Figure S8. Steady-state kinetic plots for wild-type and mutant hASNase-3 enzymes for L-Asp-β-methyl-ester as substrate. V/E versus [substrate] plot for (A) wildtype hASNase-3, (B) DM1, (C) DM2, and (D) DM3. Activities were measured in 1 mL 50 mM Tris-Cl, 100 mM NaCl, pH 8, at 25 ℃, using a final enzyme concentration of ~ 40 nM (~ 1 μg in 1 mL; hASNase-3 M_r: 33 kDa). Here, 30-fold less enzyme was used as compared to Fig.4 (in main Text) because the enzyme is 70-fold more active with this dipeptide substrate.

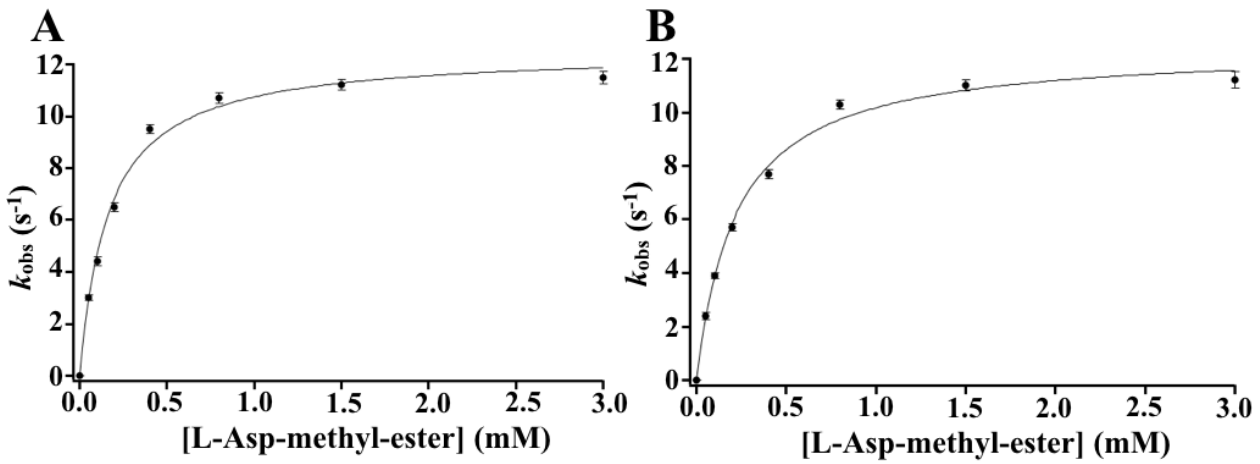

Figure S9. Steady-state kinetic plots for QDM1 and QDM2 hASNase-3 enzymes for the L-Asp-β-methyl-ester as substrate. V/E versus [L-Asp-β-methyl-ester] plot for (A) QDM1 and (B) QDM2. Reaction conditions were as shown in Fig. S8 legend above.

Table S2. Steady-state kinetic constants for wildtype and mutant hASNase-3 enzymes for L-Asp-methyl-ester hydrolysis.

Enzyme	k_{cat} (s^{-1})	K_M (mM)	k_{cat}/K_M (M^{-1} s^{-1})
wildtype hASNase3	5.4 ± 0.165	0.3 ± 0.03	18 (±2.3) x 10^3
DM1 (*Ile189Thr-Val190Ile)*	7.2 ± 0.135	0.24 ± 0.016	30 (±2.6) x 10^3
DM2 (*Ile189Val-Val190Ile)*	7.9 ± 0.21	0.24 ± 0.023	33 (±4) x 10^3
DM3 (*Arg143Glu-Arg147Lys)*	8.4 ± 0.3	0.22 ± 0.015	38.2 (±4) x 10^3
QDM1 (*Ile189Thr-Val190Ile-Arg143Glu-Arg147Lys)*	12.5 ± 0.32	0.165 ± 0.017	75.8 (±9.5) x 10^3
QDM2 (*Ile189Val-Val190Ile-Arg143Glu-Arg147Lys)*	12.4 ± 0.3	0.22 ± 0.020	56.4 (±6.5) x 10^3

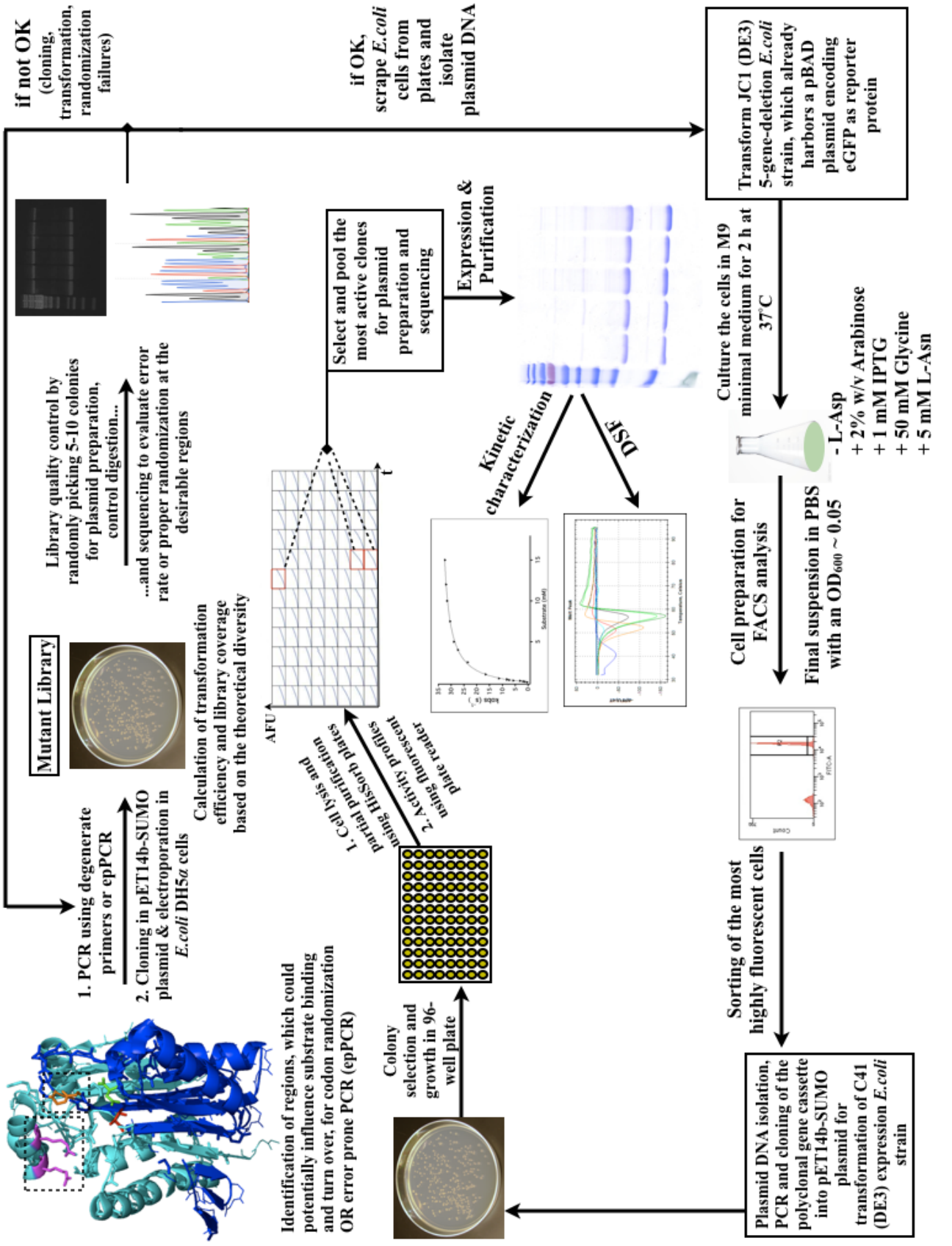

Figure S10 Overall scheme of the entire screening process starting from generation of the hASNase-3 mutant library up to the level of the kinetic characterization of the purified L-ASNase variants identified in individual sorted mutants.

REFERENCES

(1) Su, Y., Karamitros, C. S., Nomme, J., McSorley, T., Konrad, M., and Lavie, A. (2013) Free Glycine Accelerates the Autoproteolytic Activation of Human Asparaginase. *Chem. Biol. 20*, 533–540.

(2) Karamitros, C. S., Lim, J., and Konrad, M. (2014) An Amplex Red-based fluorometric and spectrophotometric assay for L-asparaginase using its natural substrate. *Anal. Biochem. 445*, 20-23.

(3) Pollegioni, L., Motta, P., and Molla, G. (2013) L-amino acid oxidase as biocatalyst: a dream too far? *Appl. Microbiol. Biotechnol. 97*, 9323-9341.

(4) Karamitros, C. S., and Konrad, M. (2014) Human 60-kDa lysophospholipase contains an N-terminal L-asparaginase domain that is allosterically regulated by L-asparagine. *J. Biol. Chem. 289*, 12962-12975.

(5) Karamitros, C. S., and Konrad, M. (2014) Bacterial co-expression of the α and β protomers of human l-asparaginase-3: Achieving essential N-terminal exposure of a catalytically critical threonine located in the β-subunit. *Protein Expr. Purif. 93*, 1-10.

(6) Cantor, J. R., Stone, E. M., Chantranupong, L., and Georgiou, G. (2009) The human asparaginase-like protein 1 hASRGL1 is an Ntn hydrolase with beta-aspartyl peptidase activity. *Biochemistry 48*, 11026 –11031.

(7) Yun, M. K., Nourse, A., White, S. W., Rock, C. O., and Heath R. J. (2007) Crystal structure and allosteric regulation of the cytoplasmic Escherichia coli L-asparaginase I. *J. Mol. Biol. 369*, 794 – 811.

(8) Swain, A. L., Jaskolski, M., Housset, D., and Wlodawer, A. (1993) Crystal structure of Escherichia coli L-asparaginase, an enzyme used in cancer therapy. *Proc. Natl Acad. Sci. USA 90*, 1474-1478.

(9) Sinclair, K., Warner, J. P., and Bonthron, D. T. (1994) The ASP1 gene of Saccharomyces cerevisiae, encoding the intracellular isozyme of L-asparaginase. *Gene 144*, 37-43

(10) Karamitros, C. S., Yashchenok, A. M., Möhwald, H., Skirtach, A. G., and Konrad, M. (2013) Preserving catalytic activity and enhancing biochemical stability of the therapeutic enzyme asparaginase by biocompatible multilayered polyelectrolyte microcapsules. *Biomacromolecules 14*, 4398-4406.